Natural Products

International Edition: DOI: 10.1002/anie.201411377
German Edition: DOI: 10.1002/ange.201411377

Discovery, Structure Elucidation, and Biological Characterization of Nannocystin A, a Macrocyclic Myxobacterial Metabolite with Potent Antiproliferative Properties**

*Holger Hoffmann, Herbert Kogler, Winfried Heyse, Hans Matter, Michael Caspers, Dietmar Schummer, Christine Klemke-Jahn, Armin Bauer, Geraldine Penarier, Laurent Debussche, and Mark Brönstrup**

Dedicated to Professor Gerhard Seibert

Abstract: *Microbial natural products are a rich source of bioactive molecules to serve as drug leads and/or biological tools. We investigated a little-explored myxobacterial genus, Nannocystis sp., and discovered a novel 21-membered macrocyclic scaffold that is composed of a tripeptide and a polyketide part with an epoxyamide moiety. The relative and absolute configurations of the nine stereocenters was determined by NMR spectroscopy, molecular dynamics calculations, chemical degradation, and X-ray crystallography. The compound, named nannocystin A (**1**), was found to inhibit cell proliferation at low nanomolar concentrations through the early induction of apoptosis. The mode of action of **1** could not be matched to that of standard drugs by transcriptional profiling and biochemical experiments. An initial investigation of the structure–activity relationship based on seven analogues demonstrated the importance of the epoxide moiety for high activity.*

Natural products have been—and continue to be—a rich source of new drugs.[1] Their contribution to the current therapy of infectious and tumor-related diseases has been particularly important: the majority of antibacterial and cytotoxic antitumor drugs are either unmodified secondary metabolites or derivatives thereof.[2] In a research project directed at the identification of novel lead compounds from natural sources, we investigated metabolites from myxobacteria, motivated by the impressive track record of this bacterial order for the biosynthesis of structurally diverse and bioactive chemical matter.[3] The best-studied compound class comprises the tubulin-stabilizing epothilons, which have yielded a clinically approved anticancer drug (Ixabepilone). Argyrins, soraphens, and disorazols are three other examples that illustrate the utility of myxobacterial products in drug discovery and for deciphering intriguing cellular biology. While the great majority of myxobacterial products has been isolated from *Sorangium cellulosum*, *Myxococcus xanthus*, and *Chondromyces* sp.,[4] only few metabolites have been described from *Nannocyctis* sp., including relatively common volatiles and siderophores and the recently discovered phenylnannolones and pyrronazols.[5] We were therefore pleased to detect a structurally novel and highly bioactive metabolite in a culture broth of *Nannocyctis* sp. ST201196 (DSM18870).[6] In this report, the isolation of the compound, the elucidation of its macrocyclic scaffold, including the relative and absolute stereochemistry, the characterization of its potent anticancer properties, and initial structure-activity relationship (SAR) studies are described.

The strain ST201196 was isolated from a soil sample. On solid media, ST201196 formed orange-yellow fruiting bodies that contained round myxospores, while the vegetative cells of the strain had a characteristic rod shape. The strain was cultivated in 2 L Erlenmeyer flasks on a 90 L scale in the presence of XAD16 adsorber resin for 7 days. A component with a molecular mass of 816.3 Da for the protonated ion and containing two chlorine atoms according to the isotope distribution pattern could not be matched to known natural products in SciFinder and DNP database searches and was therefore selected for isolation by preparative chromatography (see the Supporting Information). After freeze drying, 80 mg of **1** was obtained in more than 95% purity as an

[*] Prof. Dr. M. Brönstrup
Current address: Department of Chemical Biology
Helmholtz Zentrum für Infektionsforschung
Inhoffenstr 7, 38124 Braunschweig (Germany)
E-mail: mark.broenstrup@helmholtz-hzi.de
Dr. H. Hoffmann, Priv.-Doz. Dr. H. Kogler, Dipl.-Ing. W. Heyse, Dr. H. Matter, Dr. M. Caspers, Prof. Dr. D. Schummer, Dr. C. Klemke-Jahn, Dr. A. Bauer, Prof. Dr. M. Brönstrup
Sanofi R&D, Industriepark Hoechst
65926 Frankfurt (Germany)
Dr. G. Penarier, Dr. L. Debussche
Sanofi R&D
13 Quai Jules Guesde, Vitry sur Seine 94403 (France)
Prof. Dr. D. Schummer
Current address: TH Mittelhessen
Wiesenstraße 14, 35390 Gießen (Germany)
Priv.-Doz. Dr. H. Kogler
Current address: Institut für Analytische Chemie
Universität Bremen
Leobener Str. NW IIC 28359 Bremen (Germany)

[**] The authors thank Sandor Boros for providing his version of the hsqmbc NMR sequence.

Supporting information for this article (including experimental details) is available on the WWW under http://dx.doi.org/10.1002/anie.201411377.

amorphous powder. The high resolution mass spectrum of **1** exhibited a quasimolecular ion at m/z 816.3388 for $[M+H]^+$ that corresponded well to a neutral molecular formula of $C_{42}H_{55}Cl_2N_3O_9$ (m/z calc. of 816.3394 for $M+H$).

The chemical topology could be determined by using NMR spectroscopy. The spin topology resulting from correlations of nuclear spins via scalar couplings (^{1}H-^{1}H correlations from COSY-spectra; ^{1}H-^{13}C and ^{1}H-^{15}N correlations from HSQC and HMBC spectra) over two or more chemical bonds essentially spanned one linear system that was connected in all but one center by NMR-accessible nuclei (H, C, N). Translation into the chemical topology was unambiguous and the associated chemical shifts were in accordance with expected ranges (see the Supporting Information). Compound **1** features a 21-membered ring system with 9 chiral centers and two double bonds. The ring system consists of a tripeptide part, containing the amino acids 3-hydroxy-valine, 3,5-dichloro-tyrosine and *N*-methyl-isoleucine, and a polyketide part with an α,β-epoxy-amide substructure. Considering the taxonomy of its producer, we named **1** nannocystin A.

The absolute configuration of the amino acids was determined by Marfey's method.[7] The acid hydrolysate (5 mg, 12% aq. HCl, 100 °C, 16 h) of **1** was derivatized with 1-fluoro-2,4-dinitrophenyl-5-L-alanine-amide (L-FDAA) or D-FDAA to afford the respective FDAA derivatives of the amino acids. A comparison of the retention times observed by LCMS to those of authentic samples of the three amino acids showed that the peptide moiety of **1** contained 3-hydroxy-L-valine, 3,5-dichloro-D-tyrosine, and *N*-methyl-L-isoleucine.

The determination of the relative stereochemistry of **1** through NOE effects (distance dependencies) and vicinal coupling constants (corresponding to the torsion angles) presented various challenges. The ring system in **1** contained six quaternary centers, each separating the sequence of ^{1}H-^{1}H vicinal coupling constants. In addition, no long-range distances could be established from NOE effects. The temperature dependence of amide resonances (~ -11 ppb K^{-1}) excluded any hydrogen-bond stabilization of a single conformation. Therefore, most information was obtained from heteronuclear coupling constants[8] and from model building based on short-range constraints from NMR (Figure S15).

For the 3D structure determination, 33 dihedral-angle constraints (from 8 homo- and 25 heteronuclear coupling constants) and 115 non-trivial distance constraints were extracted from NMR data. An initial 3D model of **1** was generated from the linear structure (by replacing the ester bond by a distance constraint). Starting with the stereocenter at C5, the macrocycle was modelled by consecutively introducing distance and torsion-angle constraints for every center. For each stereocenter, both epimers were evaluated with respect to their agreement to experimental data.

After exploring both possibilities for each center through restrained molecular dynamics (MD) calculations, the configuration with better fit was kept in all cases. For refinement of this model, restrained simulated annealing (SA) calculations were performed. Only one of the stable configurations resulted in a good agreement to NOE-derived distances and torsion constraints (for details see the Supporting Information). Increasing the force constant for distance constraints consistently resulted in the inversion of incorrect stereocenters during simulated annealing. This has been reported for other small organic molecules[9] and provided evidence for the final configuration. The best model in terms of agreement to experimental data (Figure 1a and Scheme 1) showed a configuration of 5(*S*), 6(*R*), 11(*R*), 13(*S*), 14(*R*), 17*a*(*S*), 17*b*(*S*), 20(*R*), and 23(*S*) for the nine stereocenters.

In parallel, a structural analysis of **1** by means of X-ray crystallography was pursued. While all attempts to obtain single crystals of **1** remained unsuccessful, the methyl ether derivative **2**, prepared through methylation of the phenolic hydroxyl group of **1** (Scheme 1), gave crystalline needles from methanol solutions, thereby enabling a structure determination. After refinement by least-squares methods (minimization of $(F_o^2-F_c^2)^2$), an R-value of 0.1141 for all data was obtained. Owing to the presence of two chlorine atoms, it was possible to determine the absolute configuration by using the Flack parameter,[10] which has reference values of 0 for

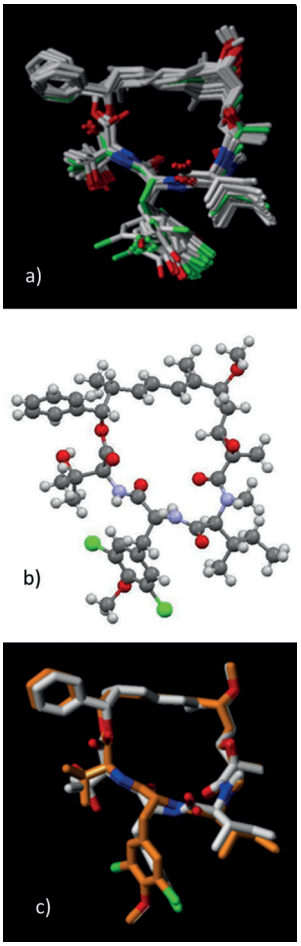

Figure 1. Structure elucidation of **1**. a) Overlay of the 22 best structures from restrained MD modelling (left) representing the NMR-derived structure. This corresponds to the configuration that was stable during simulation and best fits the experimental data. Hydrogen atoms are not shown for clarity. The least well-defined part of the molecule also shows the highest temperature variance of NMR chemical shifts. b) X-ray crystal structure of **2**.[17] c) Superposition of the X-ray (orange) and NMR (white) structures with a RMSD of the heavy atoms of 0.5 A.

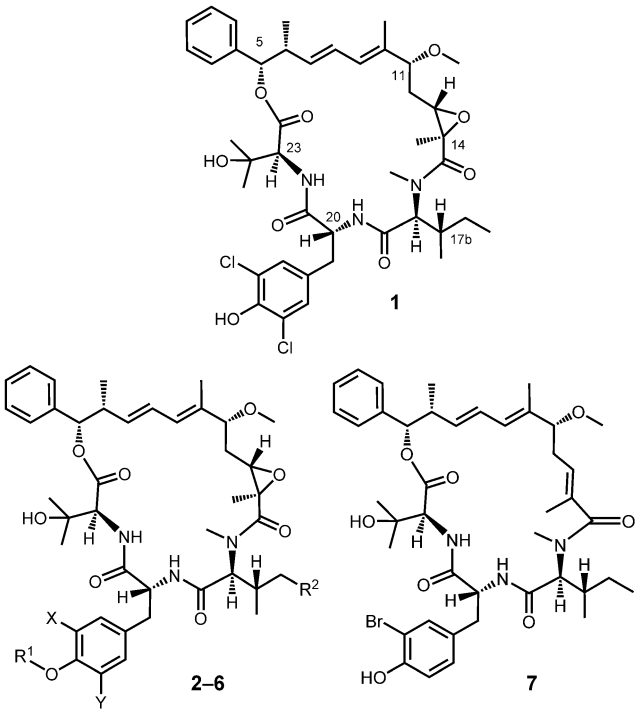

Scheme 1. Structure of nannocystin A (**1**) and its analogues.

correct and +1 for inverted absolute structures. A Flack parameter of 0.1229 was obtained for the absolute configuration depicted in Figure 1b.

The X-ray structure of **2** was in very good agreement with the NMR-derived ensemble for **1** and additionally confirmed the absence of strong hydrogen-bonding interactions (Figure 1c and the Supporting Information). The two structures differed in the observed side-chain rotamer of the 3-hydroxyvaline at C23 (χ1 dihedral angle X-ray: −163.0°, NMR: −49.0°), while geometries in all other parts of the entire structure were similar. In the peptide part, 3,5-dichloro-D-tyrosine adopted an extended β-sheet-like conformation with minor changes in the orientation of the side chain. The following *N*-methyl-L-isoleucine adopted a γi turn-like conformation (X-ray ϕ/ψ dihedral angles: −96.5°/82.3°), which was not additionally stabilized by a hydrogen bond. The geometry of the polyketide part was also well-defined and in agreement in both NMR and X-ray conformers. In conclusion, the nannocystin X-ray structure not only confirmed the independent assignment of all stereocenters, but agreed to a significant extent (with an rmsd value of 0.50 Å for all heavy atoms in the macrocycle plus all directly attached heavy atoms) with the solution structure. This indicates a stable 3D structure in different environments.[11]

We next investigated the biological activity of **1** and found that the compound had a strong antifungal effect, inhibiting the growth of *C. albicans* with a half maximal inhibitory concentration (IC_{50}) value of 73 nM.[6a] It was also a strong inhibitor of proliferation in 14 tested cancer cell lines, with IC_{50} values in the low nM range as measured by a ^{14}C thymidine incorporation assay or an ATP viability assay (Table 1 and Table S9 in the Supporting Information). Remarkably, the activity was retained against the drug-resistant cell line MDA-A1 compared to the related cell line MDA-MB231. This differentiated **1** from the reference drug docetaxel, which exhibited an approximately 2000-fold drop in activity against MDA-A1 compared to MDA-MB231 (IC_{50} values of 570 nM and 0.3 nM, respectively). Compound **1** was also active against quiescent peripheral blood lymphocytes (PBLs), thus indicating that **1** interferes with a process that is essential for basal cell metabolism. In further experiments, the ability of **1** to induce apoptosis and its effect on the cell cycle was investigated (Figure 2). Annexin V staining in the HCT116 cell line revealed that **1** is a strong inducer of apoptosis at an early time-point of 24 h, with a half maximal effective concentration (EC_{50}) value of 25 nM. Flow cytometry cell-cycle analysis showed that **1** leads to a dose-dependent increase in the subG1 population (which indicates cells in an apoptotic state)[12] in HCT116 cells, with an EC_{50} value of 20 nM.

Table 1: Antiproliferative activity of **1**.

Cell line	IC_{50} (nM)	Cell line	IC_{50} (nM)
MDA-MB231	6.5	HCT116	1.2
MDA-A1	12	PC3	1.0
PBL	11	HL60	12

Although the nannocystin scaffold has no precedence in the scientific literature, structural similarity to seragamide,[13] chondramide,[14] and jasplakinolide[15] was noted. These compounds display similar ring sizes (21 vs. 18, 18, and 19 atoms, respectively) and a mixed polyketide/tripeptide structure with a halogenated aromatic amino acid at the second position (Scheme S1 in the Supporting Information). Since all three compounds were reported to stabilize actin, the effect of **1** on F-actin was investigated by confocal microscopy in HeLa cells. However, **1** did not alter the actin cytoskeleton at

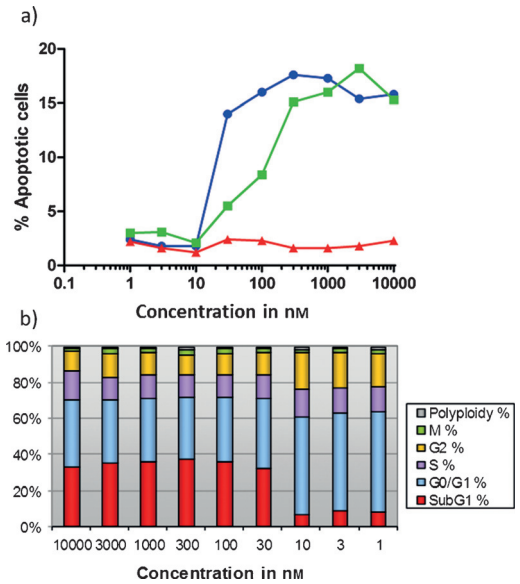

Figure 2. Cellular activity of **1**. a) Induction of apoptosis in HCT116 cells after 24 h. Blue: **1**, green: camptothecin (a cytotoxic topoisomerase inhibitor), red: inactive control substance. b) Cell-cycle analysis in HCT116 cells after 24 h. Color coding of subpopulations: red SubG1, blue G0/G1, purple S, yellow G2, green M, gray polyploidy.

concentrations up to 300 nM (Figure S2 in the Supporting Information). Furthermore, the polyploidy effects induced by other actin binders were not observed with **1**. We therefore conclude that **1** is not an actin binder. Likewise, **1** did not bind to tubulin up to a concentration of 25 μM and did not inhibit the activity of 27 kinases in ATP-competitive functional assays with purified proteins and 30 receptors (see the Supporting Information) at 10 μM. Transcriptional profiling of **1** led to a signature that did not closely match any of the other reference drugs; the closest neighbors were the proteasome inhibitors MG-132 and bortezomib (see the Supporting Information). We also noted that epoxomicin, a natural product with an epoxy keto group related to that in **1**, is a known proteasome inhibitor.[16] We therefore tested whether **1** inhibited TNFα-induced NFκ-B translocation, a hallmark of proteasome inhibitors, but did not observe an effect. In conclusion, **1** was found to be a strong inhibitor of cellular proliferation through the induction of apoptosis at an early time point. Although we described the phenotype induced by **1** and could exclude several cellular mechanisms, its precise molecular target remains to be deciphered.

An initial SAR of nannocystin was carried out with the semisynthetic analogue **2** and the fermentation products **3**–**7** (Scheme 1, Table 2, and the Supporting Information). With respect to antiproliferative activity against the HCT116 cell line, substitutions of the chlorine atoms for bromine or hydrogen at the tyrosine residue led to almost equipotent compounds. Likewise, methylation of the phenolic hydroxy group (as in **2**) or exchange of Ile for Val (**1** vs. **3**) did not affect activity. By contrast, the epoxide moiety was important for high activity, as demonstrated by analogue **7**.

Table 2: Antiproliferative activities of **1**–**7** against the HCT116 cell line.

Compound	X[a]	Y[a]	R1[a]	R2[a]	IC_{50} (nM)
1	Cl	Cl	H	Me	0.6
2	Cl	Cl	Me	Me	0.6
3	Cl	Cl	H	H	0.7
4	Cl	Br	H	Me	0.4
5	Cl	H	H	Me	0.3
6	Br	H	H	Me	0.3
7	Br	H	H	Me	$\gg 2$[b]

[a] See Scheme 1. [b] Contamination of **7** with 10–15% of **6** prevented a precise IC_{50} determination.

In summary, we report a novel natural product core structure from *Nannocystis* sp., a myxobacterial genus that has not been known as a prolific producer of secondary metabolites. The challenge to determine the relative configuration of all of the stereocenters was solved through a combination of NMR and modelling, and the result was confirmed by X-ray crystallography as an orthogonal method. The product, named nannocystin A, features a highly original structure with an unusual α,β-epoxyamide motif and high antiproliferative activity. The compound represents a novel lead structure that 1) is a promising starting point for optimization to a drug and 2) serves as a chemical pointer to a potentially novel and relevant pathway involved in cellular proliferation. The next crucial steps on these routes are the provision of a synthetic access to **1** and its analogues and the elucidation of its molecular mechanism of action.

Keywords: apoptosis · antiproliferative agents · drug discovery · natural products · structure elucidation

How to cite: *Angew. Chem. Int. Ed.* **2015**, *54*, 10145–10148
Angew. Chem. **2015**, *127*, 10283–10286

[1] A. Bauer, M. Brönstrup, *Nat. Prod. Rep.* **2014**, *31*, 35–60.
[2] a) D. J. Newman, G. M. Cragg, *J. Nat. Prod.* **2012**, *75*, 311–335; b) G. M. Cragg, P. G. Grothaus, D. J. Newman, *Chem. Rev.* **2009**, *109*, 3012–3043; c) M. S. Butler, M. A. Blaskovich, M. A. Cooper, *J. Antibiot.* **2013**, *66*, 571–591.
[3] K. J. Weissman, R. Müller, *Nat. Prod. Rep.* **2010**, *27*, 1276–1295.
[4] a) K. J. Weissman, R. Müller, *Bioorg. Med. Chem.* **2009**, *17*, 2121–2136; b) K. Gerth, S. Pradella, O. Perlova, S. Beyer, R. Müller, *J. Biotechnol.* **2003**, *106*, 233–253.
[5] a) S. M. Bouhired, M. Crusemann, C. Almeida, T. Weber, J. Piel, T. F. Schaberle, G. M. Konig, *ChemBioChem* **2014**, *15*, 757–765; b) R. Jansen, S. Sood, V. Huch, B. Kunze, M. Stadler, R. Muller, *J. Nat. Prod.* **2014**, *77*, 320–326.
[6] a) H. Hoffmann, C. Klemke-Jahn, D. Schummer, H. Kogler, in WO 2009/003595, **2009**; b) H. Hoffmann, M. Caspers, D. Schummer, H. Kogler, C. Klemke-Jahn, in WO 2010/069850, **2010**.
[7] a) P. Marfey, *Carlsberg Res. Commun.* **1984**, *49*, 591–596; b) K. Fujii, Y. Ikai, T. Mayumi, H. Oka, M. Suzuki, K. Harada, *Anal. Chem.* **1997**, *69*, 3346–3352; c) K. Fujii, Y. Ikai, H. Oka, M. Suzuki, K.-I. Harada, *Anal. Chem.* **1997**, *69*, 5146–5151.
[8] K. Kobzar, B. Luy, *J. Magn. Reson.* **2007**, *186*, 131–141.
[9] a) M. Reggelin, H. Hoffmann, M. Köck, D. F. Mierke, *J. Am. Chem. Soc.* **1992**, *114*, 3272–3277; b) H. Matter, M. Knauf, W. Schwab, E. F. Paulus, *J. Am. Chem. Soc.* **1998**, *120*, 11512–11513.
[10] H. D. Flack, G. Bernadinelli, *Acta. Crystallogr. Sect. A* **1999**, *55*, 908–915.
[11] a) M. P. Williamson, D. H. Williams, *J. Am. Chem. Soc.* **1981**, *103*, 6580–6585; b) A. K. Saksena, M. J. Green, H.-J. Shue, J. K. Wong, A. T. McPhail, P. M. Gross, *Tetrahedron Lett.* **1985**, *26*, 551–554.
[12] M. Kajstura, H. D. Halicka, J. Pryjma, Z. Darzynkiewicz, *Cytometry Part A* **2007**, *71A*, 125–131.
[13] C. Tanaka, J. Tanaka, R. F. Bolland, G. Marriott, T. Higa, *Tetrahedron* **2006**, *62*, 3536–3542.
[14] F. Sasse, B. Kunze, T. M. A. Gronewold, H. Reichenbach, *J. Natl. Cancer Inst.* **1998**, *90*, 1559–1563.
[15] a) M. R. Bubb, A. M. J. Senderowicz, E. A. Sausville, K. L. K. Duncan, E. D. Korn, *J. Biol. Chem.* **1994**, *269*, 14869–14871; b) M. R. Bubb, I. Spector, B. B. Beyer, K. M. Fosen, *J. Biol. Chem.* **2000**, *275*, 5163–5170.
[16] K. B. Kim, C. M. Crews, *Nat. Prod. Rep.* **2013**, *30*, 600–604.
[17] Supplementary crystallographic data for this paper have been deposited under CCDC 1035741. These data can be obtained free of charge from The Cambridge Crystallographic Data Centre via www.ccdc.cam.ac.uk/data_request/cif.

Received: November 24, 2014
Revised: April 20, 2015
Published online: June 1, 2015

